Free Rocking of Prismatic Blocks

By P. R. Lipscombe[1] and S. Pellegrino[2]

Abstract: This paper investigates both experimentally and theoretically the free rocking of a prismatic block supported by a stationary, horizontal foundation: the block is tilted, almost to the point of overturning, and released from this position. It is shown that the standard mathematical model for this problem is often inaccurate. A critical review of the implicit assumptions behind the standard model reveals that the free-rocking response of short blocks depends crucially on bouncing after each impact; out-of-plane effects are significant in very short blocks. The response of slender blocks is found to be easier to predict. Rocking has been observed during earthquakes in structures that consist of fairly rigid, unbonded elements, e.g. stacks of graphite blocks in nuclear reactors, and ancient Greek columns, and also in slender structures with foundations unable to resist uplift.

Introduction: Simple Rocking Model (SRM)

This paper investigates the free-rocking response of a prismatic block supported by a stationary, horizontal foundation, as shown in Fig. 1. The problem we are interested in can be described, in slightly simplified terms and referring to Fig. 2, as follows. The block is rotated through a small angle $< \alpha$ about A and then released: initially, it rotates about A until it becomes vertical; at this point, B suddenly comes into contact with the foundation, while A loses contact. Then, the block continues to rotate in the same sense, but about B; its angular velocity decreases gradually, until it becomes zero, at which point the reverse motion begins. This cycle comes to an end when the block becomes vertical and starts to rotate again about A. Because some energy is dissipated in each impact, the amplitude of the motion is gradually reduced, until the block comes to rest after a series of cycles.

This problem has practical relevance because a broadly similar response has been observed, during earthquakes, in slender water tanks and petroleum cracking towers (Housner 1956), ancient Greek and Roman stone temples (Fowler and Stillwell 1932), and stacks of graphite blocks in the core of nuclear reactors (Olsen et al. 1976). Of course, during an earthquake the foundation does not remain stationary, and hence earthquake-induced oscillations are more complex; a good understanding of the free-rocking response is essential before going on to forced rocking, as we shall discuss. In this paper we show that the deceptively simple response just described is actually quite hard to model accurately.

Following Housner (1963), let us consider the uniform block shown in Fig. 1, with mass M and moment of inertia I about its center of mass G, subject to gravity. In the simple rocking model (SRM) it is assumed that the motion of the block is essentially two-dimensional, as in the foregoing

[1]Engr., Murray-North Ltd., 106 Vincent St., Auckland, New Zealand.
[2]Lect., Dept. of Engrg., Univ. of Cambridge, Trumpington St., Cambridge, England, CB2 1PZ.

Note. Discussion open until December 1, 1993. To extend the closing date one month, a written request must be filed with the ASCE Manager of Journals. The manuscript for this paper was submitted for review and possible publication on December 1, 1991. This paper is part of the ***Journal of Engineering Mechanics***, Vol. 119, No. 7, July, 1993. ©ASCE, ISSN 0733-9399/93/0007-1387/$1.00 + $.15 per page. Paper No. 3038.

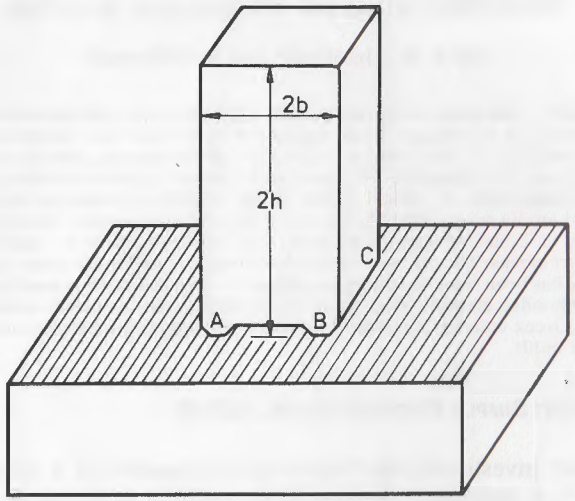

FIG. 1. View of Prismatic Block on Horizontal Foundation

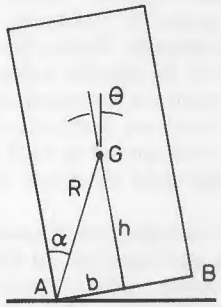

FIG. 2. Side View of Block; Rotation Angle θ is Positive in Sense Shown

description and in Fig. 2, and that the block is always in contact with the foundation, either at A, for $\theta > 0$, or at B, for $\theta < 0$: the rotation angle θ is the only degree of freedom of this system. During free-rocking tests, $|\theta/\alpha| < 1$ to avoid overturning of the block, but this value can be exceeded if the foundation is not stationary. For $\theta \neq 0$ the equation of motion, obtained simply by taking moments about the contact point, is:

$$(I + MR^2)\ddot{\theta} \pm MgR \sin(\alpha \mp \theta) = 0 \quad \ldots\ldots\ldots\ldots\ldots\ldots\ldots\ldots (1)$$

where the upper and lower signs correspond to configurations with $\theta > 0$ and $\theta < 0$, respectively.

The second term in this differential equation is nonlinear in two respects. First, the trigonometric term introduces a mild nonlinearity; in most cases, though, the approximation $\sin(\alpha - \theta) \cong (\alpha - \theta)$ is sufficiently accurate. The second cause of nonlinearity is the sudden sign change of the restoring couple when $\theta = 0$, see Fig. 3. This sign change corresponds to a discontinuity in the response of the block: when $\theta = 0$ both A and B are in contact with the foundation, and hence neither equation is valid. Actually, when θ

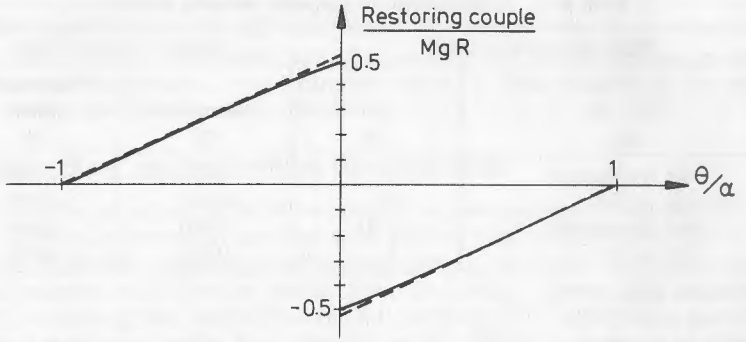

FIG. 3. Nonlinearity of Second Term in (1) for Block with $h/b = 2$

$= 0$ the block collides with the foundation: a separate analysis of this process is required. Each collision dissipates some kinetic energy, both by plastic deformation and by energy radiation into the foundation. These dissipation mechanisms provide effective forms of damping. Assuming that the collision is inelastic, i.e. that there is no bouncing, the angular velocity immediately after the impact $\dot{\theta}''$ can be calculated from the angular velocity immediately before the same impact, $\dot{\theta}'$, by equating the moment of momentum about B before the impact to the moment of momentum about the same point immediately after the impact (the moment of momentum about B is conserved because the impulsive reactions applied by the foundation act through B)

$$\dot{\theta}'(Mh^2 - Mb^2 + I) = \dot{\theta}''(Mh^2 + Mb^2 + I) \quad \ldots\ldots\ldots\ldots\ldots\ldots (2)$$

One can introduce an angular velocity ratio r, which, for the rectangular block of Fig. 1, has the remarkably simple expression

$$r = \frac{\dot{\theta}''}{\dot{\theta}'} = \frac{2h^2 - b^2}{2h^2 + 2b^2} \quad \ldots\ldots\ldots\ldots\ldots\ldots\ldots\ldots\ldots\ldots\ldots\ldots (3)$$

Note that with the preceding kinematic assumptions about the type of impact, the value of r depends only on the slenderness h/b of the block.

Unfortunately, the rather limited experimental evidence available so far suggests that the actual response of a rocking block often departs significantly from any predictions based on SRM. Aslam et al. (1980) tested concrete blocks with slightly concave bases in a series of free-rocking experiments, and also integrated numerically the equations of motion, reducing $\dot{\theta}$ by the ratio r each time the block went through the vertical position; but they had to adjust r to obtain a good match between the numerical simulation and the measured response. Their experiments were quite repeatable, but the values of r required in the simulations turned out to be quite different from those given by (3). A similar discrepancy was noted by Priestley et al. (1978), who stated that "The value of $r = 0.87$ was adopted to provide a best fit with the experimental data, and is substantially different from the value $r = 0.70$ [based on conservation of angular momentum]. It is apparent that the impacts were not totally inelastic." Table 1 summarizes the findings of three independent sets of experiments. Some discrepancies may seem deceptively small, because r is fairly insensitive to h/b when, say,

TABLE 1. Comparison of Angular Velocity Ratios

Block Dimensions (mm)		Angular Velocity Ratio	
$2h \times 2b$ (1)	h/b (2)	Measured (3)	Predicted by SRM (4)
Not rectangular[a]	2	0.870	0.700
914 × 229[b]	4	0.925	0.912
Not rectangular[c]	4.33	0.960	0.944
762 × 152[b]	5	0.925	0.942

[a]Priestley et al. (1978).
[b]Aslam et al. (1980).
[c]Muto et al. (1960).

$h/b > 4$. Actually, even in the block with $h/b = 4$ the experimentally based angular-velocity ratio corresponds to a block nearly 10% taller.

With one exception, the values of r based on the experiments are larger than those predicted by (3). Many authors (Priestley et al. 1978; Aslam et al. 1980; Spanos and Koh 1984; Tso and Wong 1989; Yim and Lin 1991) have used modified values of r in their simulations, without questioning the theoretical basis of such an approach: having made several assumptions when setting up SRM about the type of impact, about the absence of sliding and of flexural vibrations, etc., the corrected value of r tries to make allowance for them all. Although probably acceptable for an engineering solution to a specific problem, this approach could well miss out completely some important features of the response of the block, and hence turn out to produce unacceptable results when a new problem different from those for which these corrections were established is investigated.

An alternative approach was adopted by Ishiyama (1982), who set up a six-parameter two-dimensional model in which blocks can bounce up after an impact, as well as slide with respect to the foundation. This approach has not been validated experimentally and, in any case, the tangential coefficient of restitution, one of the six parameters, is not really independent. The other five parameters are a coefficient of restitution, two coefficients of friction—static and kinetic—between the edge of the block and the foundation, and two coefficients of friction between the base of the block and the foundation. This approach is not entirely correct: Stronge (1990) has pointed out that rigid-body collisions in presence of frictional sliding require a very careful analysis if slip reversal occurs during an impact. A detailed treatment of this problem is available in Shenton and Jones (1991).

A simpler model for short blocks was developed by Lipscombe and Pellegrino (1989), relying on one physical parameter, the coefficient of restitution e. The present paper shows that for slender blocks bouncing is not significant, but the second assumption of SRM, that the block behaves as a rigid body and hence at impact all of its points undergo an instantaneous change of velocity, is not always acceptable. This point is analyzed in greater detail in the section headed "Elastic Block."

In this paper we investigate in detail—both by experiment and theory—the response of four steel blocks, with $h/b = 1, 2, 4$, and 8. Our first aim, in the next section, is to find out which blocks SRM can be used reliably for. Our second aim is to establish the reasons why SRM is not accurate for some blocks, and which alternative models can be used instead. In the

section headed "Alternative Models," we introduce two- and three-dimensional rigid-body models, and also briefly discuss how the elastic flexibility of a block can be introduced into the calculations. In the section headed "Improved Predictions," we examine which of these models is the most appropriate for the four steel blocks.

Rocking Tests and Predictions Based on SRM

To test the accuracy of SRM we conducted a series of carefully monitored free-rocking experiments on four steel blocks with square cross section of 50.8 × 50.8 mm², tapering to 45.8 (average) × 50.8 mm², so that stacked configurations could also be tested. Each block had 2.5-mm-wide (average) × 50.8-mm-long feet, and all but the tallest block ($h/b = 8$) had fine parallel grooves machined under their feet, to match similar grooves on the foundation block. The function of these grooves was to prevent sliding, which would otherwise occur in short blocks (Sinopoli 1987). To a limited extent these grooves simulate a shear connector between the foundation and the block, often used in practice. When the grooves are perfectly aligned, the static coefficient of friction between block and foundation is higher than 1.3; when the grooves are not aligned, it drops to about 0.28 (this anisotropy has had some unexpected effects, discussed later). The corresponding values of the coefficient of kinetic friction are 0.16 and 0.13, respectively. Further details on the experiments are available in Lipscombe (1990).

Each block was initially tilted, almost to the point of overturning, and then released with zero angular velocity at time $t = 0$. Note that the initial rotation imparted to a block at the beginning of a free-rocking test cannot exceed α if overturning is to be avoided at the outset, hence the magnitude of the initial rotation has to be reduced as the slenderness of the block increases.

Figs. 4–7 show some typical results from these experiments. The upper part of each plot shows the rotation $\theta(t)$, measured from a series of high-speed photographs of each block (solid lines), taken from one side. The results of numerical simulations based on SRM, obtained by integrating (1) and using the angular velocity ratio r, which corresponds to the actual geometry of each block [(3)], are also shown (broken lines). The numerical implementation of SRM was based on the third-order Runge-Kutta algorithm available in Matlab (*User's* 1985). With this algorithm, (1) was integrated with a tolerance of 0.01 on the acceptable error. At the end of each rocking cycle (i.e. when the height of the other base corner had just become negative), before switching signs in (1), the block was set vertical and its angular velocity was set equal in magnitude to r times the angular velocity at the beginning of the previous cycle but in the opposite sense. (Energy is conserved while the block rotates about one corner, and hence the magnitudes of the angular velocities just after an impact and just before the following impact must be identical.) This approach turns out to be numerically more stable than referring to the last angular velocity computed—just before the impact—because this value is highly sensitive to the time step, and is sufficiently accurate only for very short time steps.

In these simulations, the initial values of θ and $\dot{\theta}$ are chosen such that: (1) The first impact occurs at precisely the same time as in the experiment; and (2) $\dot{\theta}$ before the first impact is the same as in the experiment. This results in slight variations between the experimental and theoretical initial conditions, probably due to rolling friction between the edge of the block and the foundation, significant when the block is at the beginning of its run.

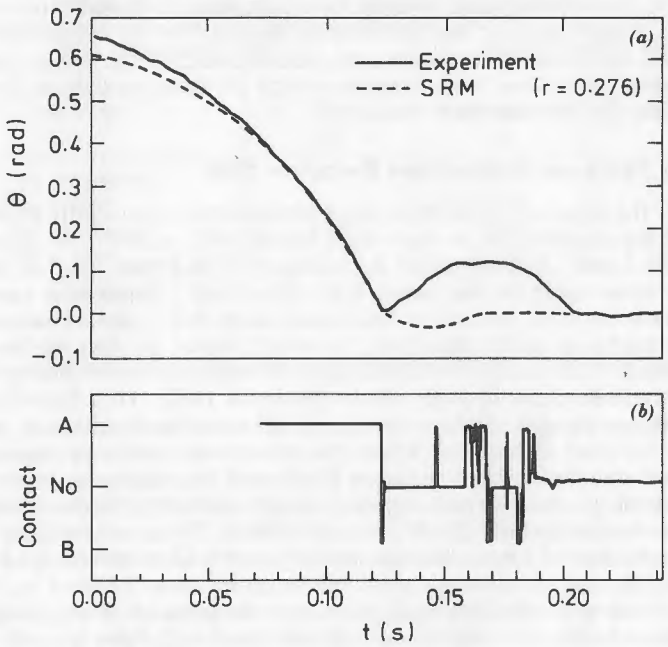

FIG. 4. Block with $h/b = 1$

Here, we shall not investigate this particular effect; from now on we shall concentrate on the response from the time when the first impact occurs.

The bottom part of Fig. 4 shows whether the block with $h/b = 1$ is in electrical contact with particular areas of the foundation. Similarly, the bottom parts of Figs. 5(*b*), 6(*b*), and 7(*b*) show whether edge B of the blocks with $h/b = 2$, 4, and 8 are in contact with the foundation. Details of the wiring diagrams from which these plots were generated are given in Lipscombe (1990). These plots provide valuable additional information on the response of the block, as discussed in the following.

The first block ($h/b = 1$), Fig. 4, has an angular velocity $\dot{\theta}' = -10.5$ rad/s just before the first impact. A sudden change occurs when $\theta = 0$ at $t \cong 0.12$ s, after which the angular velocity becomes $\dot{\theta}'' = 4.0$ rad/s. SRM gives a completely different result: $r = 0.276$ and hence $\dot{\theta}'' = r\dot{\theta}' = -2.90$ rad/s: even the direction of motion is predicted incorrectly. The plot of electrical contact shows that, after the impact at B, which lasts 180 μs, the block becomes airborne for 22 ms, it then impacts at A, and so on. Fig. 8, based on a series of high-speed photographs, shows quite clearly that this block becomes airborne after the first impact. Because bouncing forms a major part of the response, we shall need to analyze it properly: the motion of the block with $h/b = 1$ cannot be described in terms of a rotation about its base edges, hence thinking about simple rocking motion is quite misleading. An important observation, further discussed in the section headed "Improved Predictions," is that in the particular experiment from which the curve $\theta(t)$ shown in Fig. 4 was plotted the block ended up rotated about a vertical axis, its base grooves forming an angle of a few degrees with the grooves in the foundation block. This experiment has been repeated many times. In about 50% of cases the block ended up perfectly square with the

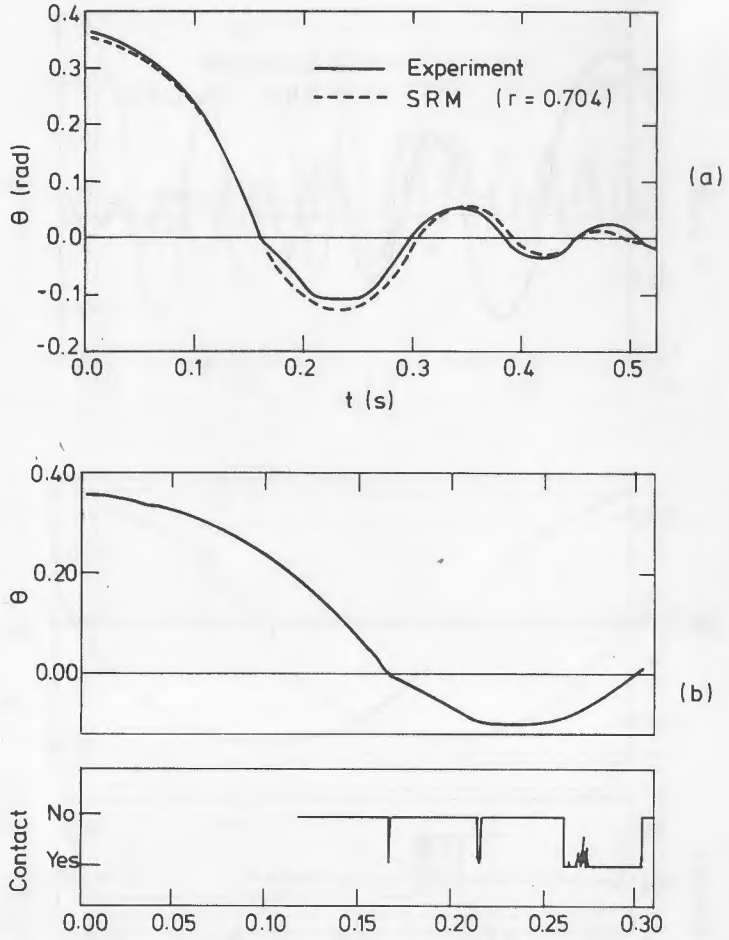

FIG. 5. Block with $h/b = 2$: (*a*) Measured and Predicted Responses during Free-Rocking Test; (*b*) Enlarged View of First Rocking Cycle, with Plot of Electrical Contact between Edge B of Block and Foundation

base, and firmly gripped by the grooves; in the remaining cases it rotated to some extent; the final rotation angle was in the range ± 7°. Fig. 8 shows clearly that, after the first impact, the bottom right corner of the block has a horizontal component of velocity: it appears that some sliding has occurred.

The block with $h/b = 2$, Fig. 5, has $\dot{\theta}' = -5.0$ rad/s and $\dot{\theta}'' = -2.1$ rad/s, respectively, before and after the first collision. Unlike the first block, here the angular velocities before and after any impact have the same sign, hence the block does rock. The curve $\theta(t)$ predicted by SRM appears to be reasonably accurate, but a closer inspection of Fig. 5(*a*) reveals that the angular velocity ratio, which should be constant and equal to $r = 0.704$ according to SRM, in reality has the values 0.44, 0.69, and 1.07 for the first

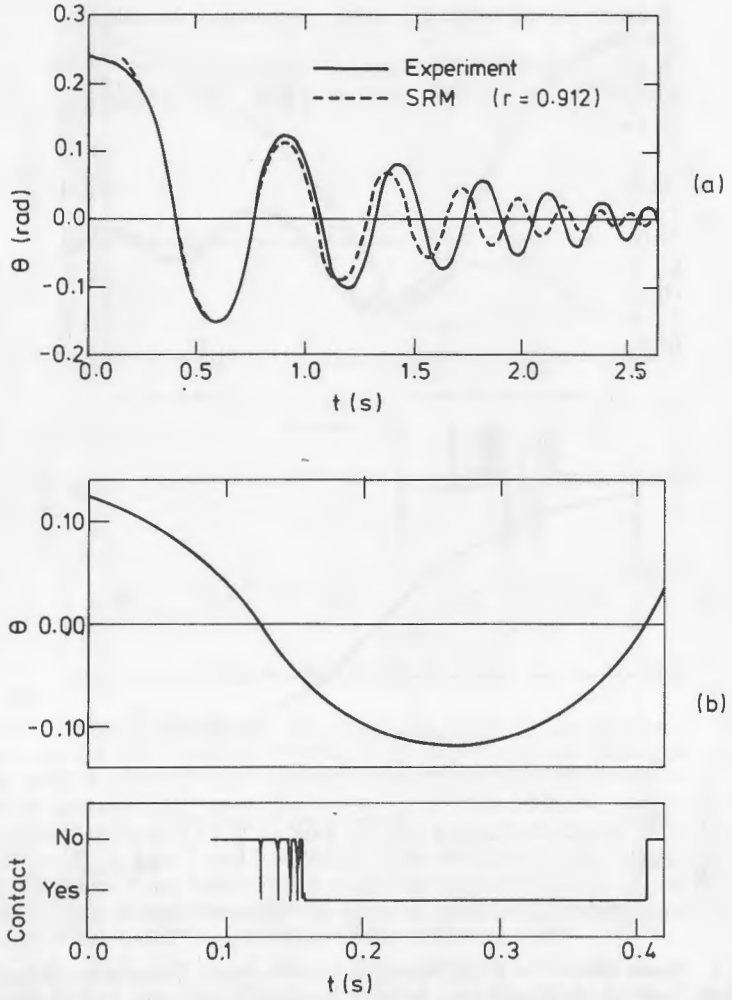

FIG. 6. Block with $h/b = 4$: Origin of Time Axis in Plot (*b*) is Different from Origin of Plot (*a*)

three collisions. Turning to the plot of electrical contact for the first bounce, Fig. 5(*b*), three well-spaced collisions have occurred, separated by bounces lasting 40–50 ms, and followed by a series of further collisions between edge B and the foundation. Then, the block stops bouncing for a short while, and B remains in contact with the foundation before the next collision at A.

The next block, with $h/b = 4$, bounces four times—see the bottom part of Fig. 6(*b*)—and then remains in contact with the foundation at B, i.e. rocks about edge B. Fig. 6(*b*) shows that the sequence of collisions plus bounces lasts less than 40 ms, while the overall period from the first collision at B to the final loss of contact, which signals the start of the next rocking phase, is about 380 ms. Bouncing would appear to be of fairly minor im-

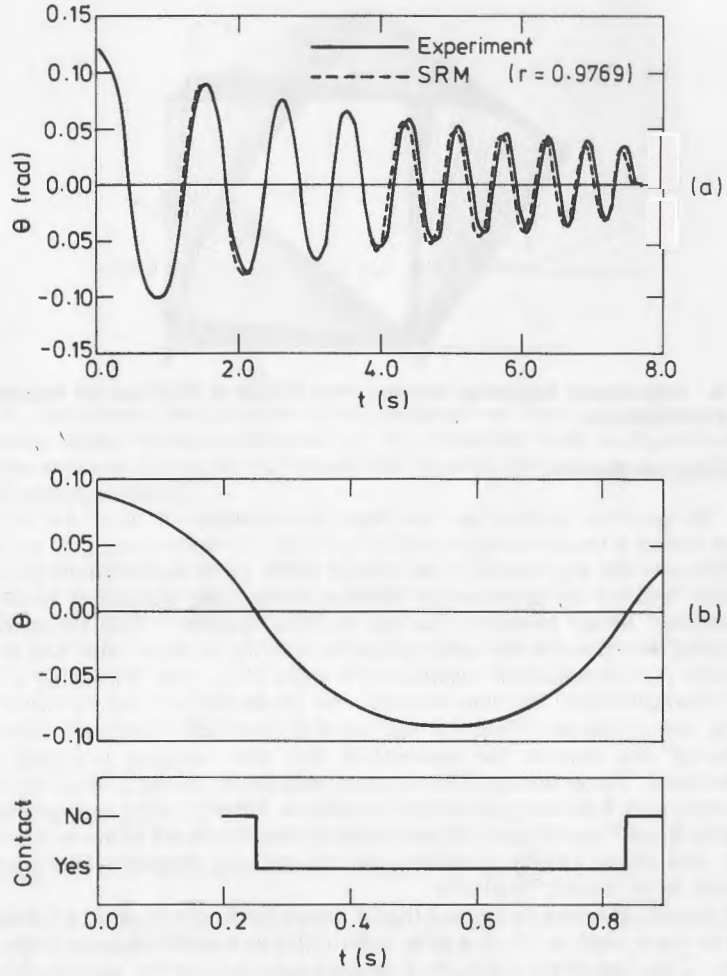

FIG. 7. Block with $h/b = 8$

portance for this block, but SRM predicts the motion to decay faster than observed; hence bouncing—or some other effect—must be significant.

The last block has $h/b = 8$. Following the first impact at B, with contact lasting 1.6 ms, the block bounces up and remains airborne for 15 ms. At the end of this bounce, the block collides again with the foundation and remains in contact with it for about 600 ms [see Fig. 7(*b*)]. In this case bouncing is definitely of minor significance, and indeed Fig. 7(*a*) shows that SRM predicts the observed response quite accurately.

The described experimental work further confirms that predictions based on SRM are usually qualitatively correct, although not quantitatively so, as indeed observed in the past by other authors. However, for the block with slenderness $h/b = 1$ we have found that the predictions are wildly inaccurate; and we have identified bouncing after each collision, which is not allowed for in SRM, as a possible cause for these inaccuracies.

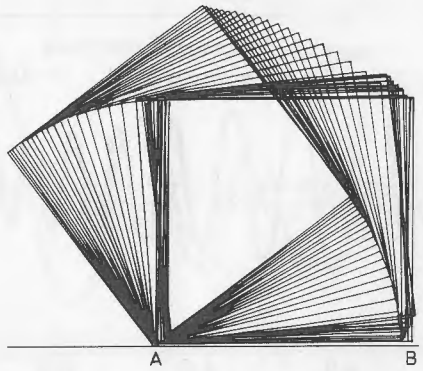

FIG. 8. High-Speed Sequence Showing that Corner B Bounces off Foundation after First Collision

Alternative Models

In the previous section we saw that the response of three out of four blocks tested is inaccurately modeled by SRM. To make progress, we gradually remove the key assumptions behind SRM, particularly that of inelastic impacts, and set up appropriate alternative models, leading to improved predictions. More precisely, in the section headed "Two-Dimensional Bouncing" we remove the assumption of inelastic impacts, and hence consider the two-dimensional response of a rigid block that, following a collision, bounces back. We also consider the possibility of unidirectional slip during the collision. Then, in the section headed "Three-Dimensional Bouncing" we remove the assumption that the response is purely two-dimensional. The resulting three-dimensional model allows a block to rotate about any axis, following an eccentric collision. Finally, in the section headed "Elastic Block" we remove the assumption that the block behaves as a rigid body, and hence briefly consider how the rocking response of a block is affected by its elastic flexibility.

Of course, it could be argued that it would be better to drop all assumptions at once, and conduct a fully comprehensive analysis using finite elements. This has been tried, to a limited extent, see the section headed "Elastic Block."

Two-Dimensional Bouncing

We wish to analyze the two-dimensional response of a block that, following a collision with the foundation, need not remain in contact with it. A general configuration of such a block is identified by three parameters, i.e. the coordinates X_G and Y_G of its centroid, plus the body rotation θ (see Fig. 9).

The response of the block consists of a series of free flights, during which the block is subject to gravity only, and—when the block collides with the foundation—the velocity components before and after the collision must satisfy an appropriate impact condition, as explained next.

The classical treatment of rigid-body collision, as described by Routh (1877), Kilmister and Reeve (1966), and by Brach (1989), assumes that the duration of contact between the two bodies is short and the interaction forces are high; hence all velocity changes can be assumed to be instanta-

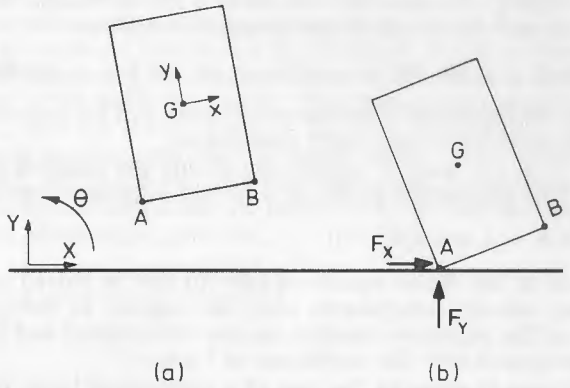

FIG. 9. (*a*) General Configuration of Block during Free Flight in Two-Dimensional Bouncing Model. Three Coordinates (X_G, Y_G, θ) Identify Each Configuration. (*b*) Collision between Corner A and Foundation, Showing (Positive) Impulsive Reactions Applied to Block

neous, no position changes occur while the bodies are in contact, and the effect of any other forces—gravity and inertia forces in the present case—can be neglected. With these assumptions, the velocity components of the block shown in Fig. 9(*b*), before and after the collision, are related to the impulse components F_X, F_Y by two equations involving linear momentum—in the X- and Y-directions, respectively—and moment of momentum about the centroid. The resulting system of three equations is

$$M\dot{X}''_G - F_X = M\dot{X}'_G \quad \ldots\ldots (4a)$$

$$M\dot{Y}''_G - F_Y = M\dot{Y}'_G \quad \ldots\ldots (4b)$$

$$I\dot{\theta}'' + (x_j \sin\theta + y_j \cos\theta)F_X - (x_j \cos\theta - y_j \sin\theta)F_Y = I\dot{\theta}' \quad \ldots\ldots (4c)$$

where $'$ and $''$ denote the velocity components before and after the collision, respectively; and j = impact point. For example, $(x_j, y_j) = (-b, -h)$ for impact at corner A. Because there are three unknown velocity components, namely $\dot{X}''_G$, $\dot{Y}''_G$, and $\dot{\theta}''$, as well as two unknown impulse components, system (4) by itself does not determine uniquely the conditions of the block after the collision.

There are two standard ways of obtaining two additional conditions: (1) Newton's law of impact, which imposes kinematic conditions on the normal and tangent components of the rebound velocity the impact point; and (2) the alternative, more elaborate and yet conceptually more satisfying, approach, using Poisson's decomposition of each impulse into its compression and restitution phases—the ratio between the latter and former components is equal to the coefficient of restitution e, which can be measured experimentally, see the section headed "Improved Predictions"—which produces identical results to Newton's law of impact if there is no slip or if slip is unidirectional and continues throughout the collision (Stronge 1990).

For the sake of simplicity, here we use the first approach, hence the vertical velocity component, after an impact, of the corner that collides with the foundation is a constant proportion of the same component of velocity

before that impact. The ratio between them is the coefficient of restitution e ($0 \le e \le 1$), and this results in the kinematic condition

$$\dot{Y}''_G + (x_j \cos\theta - y_j \sin\theta)\dot{\theta}'' = -e[\dot{Y}'_G + (x_j \cos\theta - y_j \sin\theta)\dot{\theta}'] \quad \ldots (5)$$

Regarding the horizontal components of velocity of the impacting corner, the following three cases have been considered.

First, $\dot{X}''_j = 0$, i.e. there is neither slip during the collision nor velocity restitution. This assumption results in a further kinematic condition

$$\dot{X}''_G - (x_j \sin\theta + y_j \cos\theta)\dot{\theta}'' = 0 \quad \ldots (6)$$

The system of five linear equations (4)–(6) can be solved uniquely for the unknown velocity components after the impact. In the process, the components of the impulsive reaction are also determined and the ratio F_X/F_Y can be compared with the coefficient of friction.

It is interesting to consider the case of a rectangular block that prior to impact rotates about edge A, as in Fig. 2. At the instant when edge B impacts with the foundation, the block lifts off the foundation at edge A, and if $e > 0$, then edge B also lifts off. The ratio between the angular velocity after the impact and that before the impact can be found from the bouncing theory just described above, and turns out to be

$$r = \frac{\dot{\theta}''}{\dot{\theta}'} = \frac{2h^2 - b^2 - 3b^2e}{2h^2 + 2b^2} \quad \ldots (7)$$

this expression agrees with (51) of Shenton and Jones (1991). In the case of a perfectly inelastic impact, that is $e = 0$, edge B remains in contact with the foundation after the impact, and the ensuing angular velocity of the block is exactly as in SRM. In the case of partially elastic impacts, that is $e > 0$, the angular velocity after the impact is always smaller than predicted by SRM.

Second, $\dot{X}''_j = -e\dot{X}'_j$, i.e. the same coefficient of restitution relates both vertical and horizontal components of velocity. The resulting kinematic condition is

$$\dot{X}''_G - (x_j \sin\theta + y_j \cos\theta)\dot{\theta}'' = -e[\dot{X}'_G - (x_j \sin\theta + y_j \cos\theta)\dot{\theta}'] \quad \ldots (8)$$

This approach attempts to capture the effects of tangential elastic compliance, investigated by Maw et al. (1981), and by Johnson (1983) for the oblique impact of a sphere on a flat plate, in a rather simplified way. The tangential coefficient of restitution can be set lower than the normal coefficient of restitution used in (5), or even negative to allow for the effect of microslip between the two surfaces. Note that although Maw et al. (1981) show that the value of the tangential coefficient of restitution depends on the angle of incidence, here we are taking it to be constant.

As in case one, solution of the system of five linear equations (4), (5), and (8) provides the velocity components after the impact.

Three, unidirectional slip occurs throughout the collision, hence

$$F_X = \pm\mu F_Y \quad \ldots (9)$$

Here μ = coefficient of kinetic friction. In this case, no additional kinematic condition is required; however, the correct sign to be used in (9) can be obtained from a preliminary analysis, assuming case one. Then, (9) can be used to eliminate F_Y, say, from equations (4) and (5), and the resulting system of four equations can be solved uniquely.

The analysis of a free flight is straightforward. The horizontal translation of the block is not required, and therefore it is neglected. $Y_G(t)$ is quadratic and because no external couples act on the block, $\theta(t)$ is a linear function that is fully defined once the configurations of the block at the beginning and at the end of the flight are known. For given initial conditions, all that is needed is to find out which corner of the block will collide next with the foundation, and how long this takes. It can be shown easily—assuming small block rotations, and hence that series expansions up to second-order terms are acceptable for the trigonometric terms—that the time interval between two successive collisions is given by

$$\Delta t = \min_j \left(\max \frac{-b_j \pm \sqrt{a_j^2 - 4a_jc_j}}{2a_j} \right) \quad \ldots (10a)$$

where

$$a_j = -0.5(g + y_j\dot{\theta}^2) \quad \ldots (10b)$$

$$b_j = \dot{Y}_G + x_j\dot{\theta} - y_j\theta\dot{\theta} \quad \ldots (10c)$$

$$c_j = Y_G + x_j\theta + y_j(1 - 0.5\theta^2) \quad \ldots (10d)$$

In these expressions all values of the coordinates and velocity components of the block refer to the beginning of the free flight. In the simulations, only two impact points have been considered, hence a free flight lasted until either A or B collided with the foundation.

To simulate the free rocking of a block with the two-dimensional bouncing model, the block is set initially vertical, with velocity components equal to those measured just before the first collision. Thus, the first collision occurs at $t = 0$ and, after the velocity components have been calculated, an analysis of the ensuing free flight yields the time of the next collision, with the corresponding configuration and velocity components of the block at that instant. Further collisions and free flights are analyzed exactly in the same way.

Three-Dimensional Bouncing

Conceptually, this model is similar to the previous one: as before, the response of the block consists of a series of collisions and free flights, which terminate when a corner of the block comes in contact with the foundation. The detailed analysis, though, is much more elaborate than in the two-dimensional case mainly because to identify a general state of the block we require, in addition to the three Cartesian coordinates of the centroid G and the corresponding translational velocity components, the three Eulerian angles and their first-order time derivatives. This gives a total of 12 parameters in the state vector

$$[X_G, Y_G, Z_G, \dot{X}_G, \dot{Y}_G, \dot{Z}_G, \Phi, \Theta, \Psi, \dot{\Phi}, \dot{\Theta}, \dot{\Psi}] \quad \ldots (11)$$

where a system of space axes has been introduced, with the X-Y plane coplanar with the foundation, and the Z-axis vertical and directed upward; the Eulerian angles follow the standard X, Y, Z convention (Goldstein 1980). Note that unlike the earlier two-dimensional analyses, the Y-axis is now horizontal. In addition, in analogy with Fig. 9(a), we also consider a set of body axes x, y, z along the principal axes of the block.

The analysis of a collision involves linear momentum in the direction of

the space axes, moment of momentum about the body axes, and kinematic conditions in the direction of the space axes, yielding the following system of nine linear equations in nine unknowns:

$$\begin{bmatrix} M & & & 0 & & & -1 & & \\ & M & & & 0 & & & -1 & \\ & & M & & & 0 & & & -1 \\ \hline & & & I_x & & & & & \\ 0 & & & & I_y & & & \mathbf{CA} & \\ & & & & & I_z & & & \\ \hline -1 & & & & & & 0 & & \\ & -1 & & & \mathbf{A}^T\mathbf{C}^T & & & \mathbf{0} & \\ & & -1 & & & & & & 0 \end{bmatrix} \cdot \begin{bmatrix} X''_G \\ Y''_G \\ Z''_G \\ \hline \omega''_x \\ \omega''_y \\ \omega''_z \\ \hline F_X \\ F_Y \\ F_Z \end{bmatrix} = \begin{bmatrix} M\dot{X}'_G \\ M\dot{Y}'_G \\ M\dot{Z}'_G \\ \hline I_x\omega'_x \\ I_y\omega'_y \\ I_z\omega'_z \\ \hline 0 \\ 0 \\ e(\dot{Z}'_G + \mathbf{A}_3^T\mathbf{C}\boldsymbol{\omega}') \end{bmatrix} \quad \ldots\ldots (12)$$

$\mathbf{A}$ = rotation matrix from space to body coordinates [see page 609 of Goldstein (1980)]; $\mathbf{A}_3$ denotes the third column of $\mathbf{A}$

$$\mathbf{C} = \begin{bmatrix} 0 & z_j & -y_j \\ -z_j & 0 & x_j \\ y_j & -x_j & 0 \end{bmatrix}$$

for impact at corner $j = (x_j, y_j, z_j)$; ω_x, ω_y, and ω_z = angular velocity components of the block, with respect to the body axes; hence $\boldsymbol{\omega}' = [\omega'_x\omega'_y\omega'_z]^T$ = angular velocity before the impact.

The first two kinematic conditions included in system (12) are based on the assumption that there is neither slip nor horizontal restitution, in analogy with case one of the section headed "Two-Dimensional Bouncing." The third kinematic condition is the version in three dimensions of (5).

In the section headed "Improved Predictions" we also consider collisions with a foundation which is frictionless in the Y-direction. This condition can be implemented quite easily: for $F_Y = 0$, (1)–(7) and (9) of system (12) determine uniquely the eight remaining unknowns. Eq. (8) can provide the slip velocity in the Y-direction after the collision.

The free-flight analysis for a three-dimensional rocking block is based on the integration of the standard Euler's equations of motion for a rigid body by a Runge-Kutta algorithm. Because a full appreciation of the detailed procedure is not required for present purposes, only an outline of the algorithm is given here.

The key point is that a Runge-Kutta algorithm requires that the time derivatives of the state vector (11) be evaluated for different values of t. Obviously, given (11) at time t, the time derivatives of the first six parameters are precisely the remaining six parameters of the state vector itself, hence no calculations are needed to find their values. Furthermore, the translational acceleration components remain constant throughout the flight, and they are $\ddot{X}_G = 0$; $\ddot{Y}_G = 0$; and $\ddot{Z}_G = -g$. Thus, only the second-order time derivatives of the Eulerian angles are to be calculated. They are obtained from Euler's equations of motion for a rigid body [Goldstein (1980), page 205], which, in the absence of external torques, simply relate ω_x, ω_y,

and ω_z, to $\dot{\omega}_x$, $\dot{\omega}_y$, and $\dot{\omega}_z$. However, first the angular velocities must be calculated from the standard relationships

$$\omega_x = \dot{\Psi} - \dot{\Phi}\sin\Theta \quad \ldots\ldots (13a)$$

$$\omega_y = \dot{\Theta}\cos\Psi + \dot{\Phi}\cos\Theta\sin\Psi \quad \ldots\ldots (13b)$$

$$\omega_z = -\dot{\Theta}\sin\Psi + \dot{\Phi}\cos\Theta\cos\Psi \quad \ldots\ldots (13c)$$

Once the angular-velocity and angular-acceleration components are known, the corresponding second-order derivatives of the Eulerian angles are the unique solution of a three-by-three system of linear equations, which is obtained by differentiation of (13).

At each step of the integration, before accepting the latest set of results, the Z-coordinates of some predefined impact points—usually the four bottom corners of the block—are calculated: if any of these coordinates are less than -0.01 mm, the latest set of results is discarded and the time step is halved. This approach has been found to work successfully in all cases tested.

The simulation of a rocking test with the three-dimensional bouncing model is conducted in a similar way to the two-dimensional simulation described at the end of the section headed "Two-Dimensional Bouncing." However, the time history thus obtained, expressed in terms of Eulerian angles, must be converted to $\theta(t)$, i.e. the block rotation as seen from a side; θ can be obtained from the X- and Y-components of a unit vector parallel to the x-axis and lying on the face of the block, which was observed during the rocking tests.

Elastic Block

So far, we have assumed that both the block and the foundation can be treated as rigid bodies, apart from the regions near the impact points, which suffer some elastoplastic deformation. This assumption greatly simplifies the analysis of a collision because the conditions on linear momentum and moment of momentum are easy to set. Obviously, we must check that this assumption is acceptable for the four blocks whose behavior we are investigating. In general, it would be good to know in what range of block slenderness rigid-body models can be used confidently.

It is easy to deal with the first point, since the rigid-body assumption is acceptable when the duration of a collision is sufficiently long to allow several reflections of the waves associated with the impact (Goldsmith 1960) or, equivalently, it is long in comparison with the fundamental natural period of the block. It can be seen from Table 2 that this condition is satisfied by all four blocks. Table 2 shows the measured duration of the first collision of each block, from the section headed "Rocking Tests and Predictions Based

TABLE 2. Measured Contact Duration and Fundamental Periods

h/b (1)	Contact duration (μs) (2)	Fundamental period (μs) (3)
1	180	16
2	240	35
4	520	140
8	1,600	500

on SRM," and the measured fundamental periods—details on the latter experiments are given by Lipscombe (1990). The fundamental periods of the first two blocks are predicted rather accurately by considering the time taken by an axial wave to travel the full height of the block and back to the base. On the other hand, for the blocks with $h/b = 4$ and 8, the measured fundamental period is near to the period of the first bending mode in a free-free beam: the values estimated thus are, respectively, only 17% and 4% lower than the experimental values in Table 2. Because no less than three complete oscillations would take place during these collisions, it can be concluded that the experiments discussed in this paper have not been influenced by the overall elastic deformation of the blocks. This has been further confirmed by conducting rocking tests on two acrylic blocks, with $h/b = 4$ and 8: in spite of a wave speed about 2.5 times lower than steel, they behaved almost identically to steel blocks with equal slenderness. From Table 2, the trend is that the rocking response of steel blocks with $h/b > 15$ should begin to show the effects of their overall deformation.

A qualitative understanding of how overall deformation can affect the response of a block can be gained from the simple two-block model introduced by Lipscombe and Pellegrino (1989): the original block is split into two smaller blocks of height h_1 and h_2, with $h_1 + h_2 = 2h$, which are connected by a frictionless cylindrical hinge and by a linear-elastic rotational spring. An SRM-type analysis of this model reveals an angular velocity ratio that is always larger than the value given by (3). Therefore, the energy loss in each collision is reduced and the motion decays at a slower rate. With models of this type there is an obvious difficulty in choosing rationally the value of h_1/h_2 and the spring constant. For quantitative estimates one can do a finite-element analysis of the collision between a block and the foundation. Lipscombe (1990) used the dynamic linear-elastic option of MARC (1988) to analyze a block with $h/b = 8$. The block was modeled by eight-node rectangular plane-strain elements and the foundation by two linear-elastic springs without damping, thus simulating a perfectly elastic impact. The resulting simulation of the first collision was quite disappointing, mainly because the first collision during the free-rocking test was predicted to last about 240 μs, instead of the measured 1,600 μs, which leads to an unrealistic coupling between rigid-body response and elastic deformation of the block. Further investigation of this approach is needed, with more realistic foundation models.

Improved Predictions

In this section we reanalyze the response of the blocks with $h/b = 1$, 2, and 4 using the two bouncing models introduced in the section headed "Alternative Models." We also investigate the effects on SRM of small geometrical imperfections. First, though, we find out under which conditions a two-dimensional bouncing analysis will produce significantly different results from SRM.

For example, let us consider a block with slenderness $h/b = 4$ and, having turned it about A through $\theta = 0.24$ rad, let us analyze its response using both SRM and the two-dimensional bouncing model. Obviously, there is no difference in response until the first collision occurs, at which point SRM predicts that the block will start rocking about B; and the bouncing model predicts a series of free flights (of ever decreasing duration) separated by collisions between corner B of the block and the foundation. If $e = 0.9$, the duration of the seventh flight is about half that of the first flight. Similarly, the vertical velocity component of the impact point gradually tends to zero and, when it has become negligibly small, the motion of the block is essentially the same as rocking about corner B. The $\theta(t)$ curves predicted by these two models are practically identical over the first half-cycle if the t-axis for the curve predicted by SRM is stretched by about 2%. It can be concluded that the effect of bouncing is not significant for a block with slenderness $h/b = 4$ and coefficient of restitution $e = 0.9$. It can be easily shown that this result is independent of the initial rotation amplitude.

Fig. 10, obtained from a series of analyses of the type just described, generalizes this statement: for blocks represented by points well inside the hatched region the bouncing model is usually not required. However, points outside the hatched region, or inside it but near the boundary between the two regions, identify blocks whose response may consist entirely of bounces on one edge or the other, until they come to rest, without ever reentering the rocking regime. For such blocks, the bouncing model is more appropriate. Of course, these results are valid only if the base is stationary. If the base is shaken (e.g. by an earthquake), then the motion of a bouncing block becomes decoupled from that of the base while the block is airborne, unlike a rocking block.

To use a bouncing model, or even just Fig. 10, it is essential to know the value of the coefficient of restitution e. Although values of e for spheres of different materials, sizes, and impact velocities are available in the published literature (Goldsmith 1960), these data are of limited applicability to rocking blocks, because the geometry of the impact surfaces is markedly different in this case.

The coefficient of restitution of the blocks used in the free-rocking tests has been measured simulating the impact conditions when $\theta = 0$ (see Fig. 11) on blocks similar to those used in the rocking tests but suspended through the center of percussion. Further details on these tests are given by Lipscombe (1990). For the relatively low-impact velocities in which we are interested here, e is practically constant and equal to 0.9: it appears that there is almost no plastic deformation. With a single exception, in the section headed "Block with $h/b = 2$," the value $e = 0.9$ is used from now on.

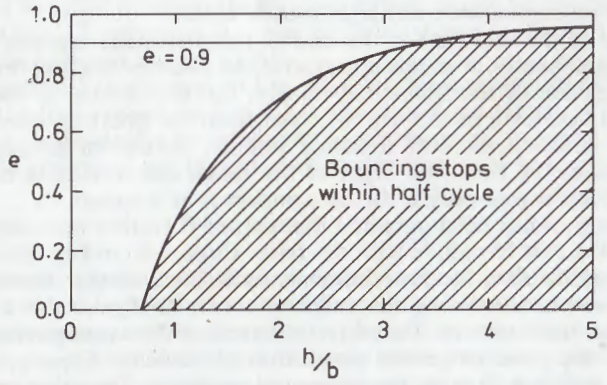

FIG. 10. SRM is Quite Accurate for Blocks Represented by Points in Hatched Region; Outside this Region Bouncing does not Stop, hence Rocking Regime does not Resume after First Collision

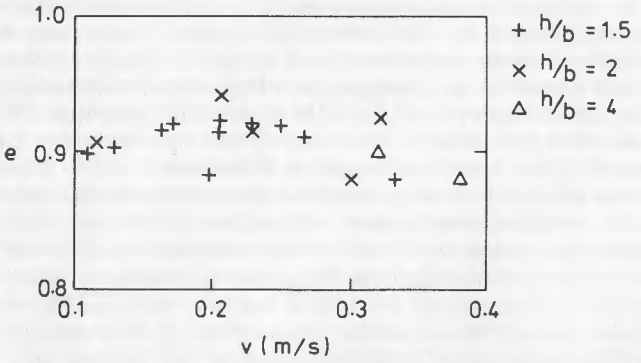

FIG. 11. Normal Coefficients of Restitution e for Steel Blocks Colliding with Steel Base; v is Approach Velocity; Only Corner Impact is Considered.

Block with $h/b = 1$

The response of this block, poorly modeled by SRM, has been reexamined with the aid of the two bouncing models. Fig. 12 shows the new results obtained thus.

Curve (ii) in Fig. 12 is predicted by the two-dimensional bouncing model, assuming (case one in the section headed "Two-Dimensional Bouncing") that there is no slip and no tangential restitution. This model predicts, correctly, that after the collision between edge B and the foundation, edge A collides twice with it.

After the first collision curve [(i)], the experimental curve and curve (ii) practically coincide (which is much better than the prediction obtained from SRM) until suddenly curve (i) becomes horizontal: it appears that the first bounce has been correctly modeled, and hence the value $r = 0.425$ obtained from (7) is correct, but that in reality the duration of the first free flight is much shorter than predicted. Many attempts have been made to improve this result, repeating the analysis with different values of e, introducing tangential restitution as well, and also considering slightly asymmetric blocks whose centroids are nearer to a base edge than to the other. However, the predicted responses were not significantly better.

In view of the fact that at the end of this particular test the block had twisted significantly, it seems appropriate to examine the full three-dimensional response of the block. Obviously, the predictions of the three-dimensional bouncing model are different from the previous ones only if at least one collision involves a corner impact, instead of an edge impact. Furthermore, the first free flight of the block can terminate earlier than previously estimated only if the first impact is at a corner.

Therefore, it has been assumed that corner B (rather than edge BC, see Fig. 1) is the first to collide with the base. Curve (iii) in Fig. 12 is based on the assumption that the foundation is frictionless in the direction of the grooves, and hence during the collision corner B slips in the Y-direction, causing the block to twist. Curve (iv) is based on the assumptions that there is neither slip, nor tangential restitution of velocity. Clearly, curve (iii) produces the best fit with the measured response. Its rather extreme kinematic assumption has been further investigated by performing additional free-rocking tests to find out if it is correct to assume that slip takes place during the first collision, and hence that the block can rotate about a vertical

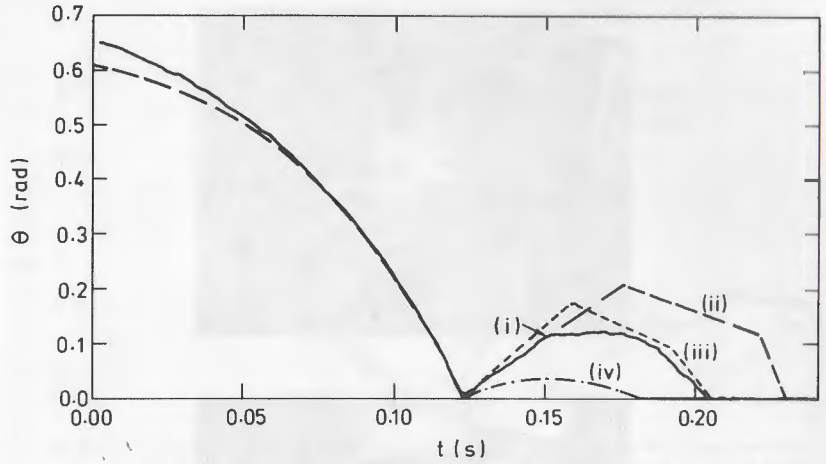

FIG. 12. Block with $h/b = 1$: Curve (i) is from a High-Speed Photographic Record of Test; Curve (ii) is Prediction from Two-Dimensional Bouncing Model; Curves (iii) and (iv) are Obtained from Three-Dimensional Bouncing Model, Assuming that First Collision Occurs at Corner B and that there is no Friction in Direction Parallel to Grooves in Base (iii), or there is no Slip (iv) (in all Cases $e = 0.9$)

axis as a result of the first collision. Fig. 13 shows two multiple-exposure photographs of a block sprayed with black paint and marked with two white crosses: the cross on the side face shows the rotation θ, while the cross on the top face shows the twist angle. These two photographs were taken with strobe light set at a rate of 50 flashes/sec. Although this photographic record is much less precise than high-speed camera films from which all $\theta(t)$ plots were obtained, it is perfectly suitable for the present qualitative investigation.

In the first test, the block does not twist, see Fig. 13(a), but in the second test, Fig. 13(b), the block twists immediately after becoming vertical. This second test supports the preceding hypothesis: because the plots in Figs. 4 and 12 refer to a test in which the block did twist, it can be concluded that curve (ii) in Fig. 12 corresponds to the behavior shown by Fig. 13(a), while curve (iii) corresponds to Fig. 13(b).

Finally, notice that although in Fig. 13(a) both crosses translate horizontally after the first impact, in Fig. 13(b) the combined effects of bouncing and sliding—probably due to a slight initial misalignment between the block and the base grooves—are that the side cross appears to have moved very little.

Block with $h/b = 2$

Fig. 14 shows, together with the measured response of this block and the response predicted by SRM, two more predictions obtained from the two-dimensional bouncing model, assuming no slip and no tangential restitution. For $e = 0.9$, the predicted response becomes quite inaccurate after the first four or five collisions; but the curve corresponding to $e = 0.89$ is better.

Other values of e in the range 0.85–0.92 have also been tried; the conclusion is that predictions from the bouncing model are very sensitive to the value of e. For example, for $e = 0.85$, the first half-cycle ($\theta < 0$) is

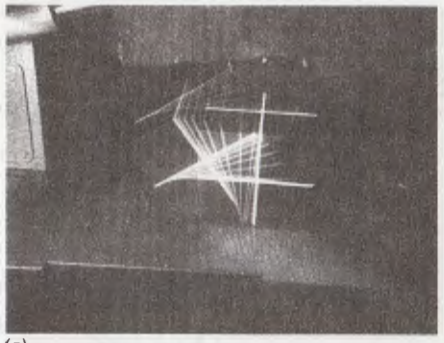

(a)

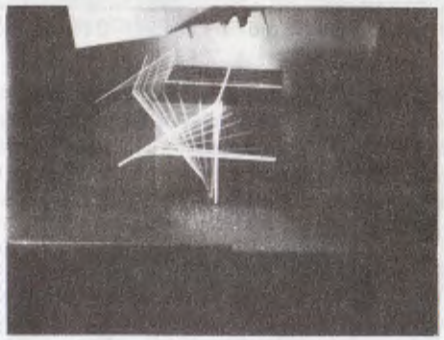

(b)

FIG. 13. Multiple-Exposure Photographs of Block with Slenderness $h/b = 1$ Taken with Strobe Light set at 50 flashes/sec: (a) Block Does not Twist; (b) Block Twists Immediately after Corner B Collides with Base, as Shown by Cross on Top Face of Block

correctly predicted, but then in the next half-cycle ($\theta > 0$) a maximum rotation $\theta \approx 0.11$ rad is reached, which is well above the value measured in the experiment.

Introduction of a horizontal coefficient of restitution does not change the results significantly over the time period of interest. Predictions from the three-dimensional bouncing model are only slightly better. For $e = 0.9$ and the first impact at corner B, the hypothesis of no slip produces the most accurate results: the first three half-cycles are predicted quite accurately, but in the fourth half-cycle $\theta_{max} = 0.045$ rad, which is much larger than found in practice. It is conceivable that this value would not be reached for a slightly different value of e, but this possibility has not been investigated.

If, instead, the block is allowed to slip in the direction of the grooves during each collision, the motion of the block dies down much more quickly than found in practice. This agrees perfectly well with the observation that no twisting occurred during the particular rocking test from which our experimental data were derived.

Block with $h/b = 4$

From Fig. 10, it is quite clear that bouncing models are not particularly useful for this block, because of the very short duration and rapid decay of

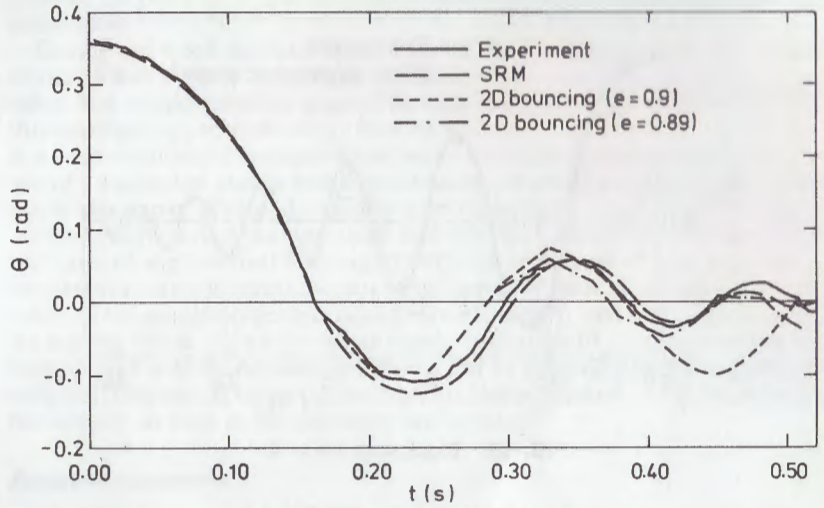

FIG. 14. Block with $h/b = 2$

the free flights that follow each collision. An interesting result, though, is obtained by letting the computer program, which models two-dimensional bounces, run for about 1,000 impacts. This provides a simulation of the first half-cycle, if rocking (i.e. $e = 0$) had been assumed instead: this $\theta(t)$ curve is practically identical to that obtained much more rapidly from SRM, provided the t-axis is stretched by about 2%. Hence, bouncing has the effect of delaying the "rocking" cycle. By itself, this effect is rather small, but it provides a (partial) explanation for the too-fast rate of decay predicted by SRM, in Fig. 6.

A further, partial, explanation is obtained by investigating the effects of small geometrical imperfections on rocking response. Lipscombe (1990) has studied how a small out-of-flatness of the base would affect the response and found that a three-dimensional rocking model that assumes corner impacts (with $e = 0$) produces results essentially identical to SRM. A more successful approach is to extend SRM to include blocks that lean to one side. Thus, the length AB $= 2b$ in Fig. 2 becomes AB $= b_1 + b_2$, and consequently AG $= R_1$ and BG $= R_2$. The revised model shows that even fairly small asymmetries slow down the response of the block. For example, Fig. 15 shows the prediction obtained for $b_1 = 22.1$ mm and $b_2 = 23.1$ mm, which is better (particularly over the first two half-cycles) than the SRM prediction for a geometrically perfect block, in Fig. 6. Note that although, strictly speaking, for asymmetric blocks both the equation of motion and the angular velocity ratio depend on the sign of θ, for $h/b = 4$ the change in the value of r has negligible consequences. Actually, the block used in the rocking tests does lean a bit, by about 0.001 rad—this value has been measured with a three-axis coordinate-measuring machine [see Lipscombe (1990)]—but this accounts for only 1/5 of the imperfection considered in Fig. 15. Of course, similar effects would have been caused by an out-of-level foundation, but, unfortunately, no data were available on the horizontality of the base block. Therefore, it can only be concluded that although the measured block asymmetry does not explain fully the discrepancy be-

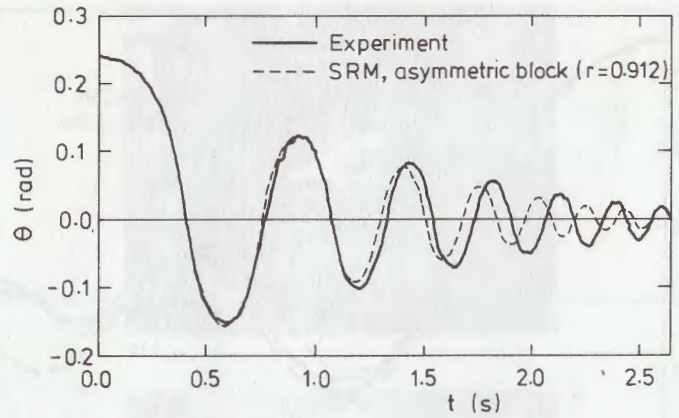

FIG. 15. Block with $h/b = 4$

tween the response of this block and the SRM prediction, this effect may have been amplified during the test by a nonlevel base.

Comment

It was shown that the apparent simplicity of a free-rocking tests can hide some rather subtle phenomena, and hence that the simple rocking model may be inadequate in some cases. Broadly speaking, SRM is adequate for slender blocks, i.e. for blocks that are represented by points in the hatched region of Fig. 10. However, if more than only one or two rocking cycles are of interest, one should be aware that the effects of small geometrical imperfections such as a nonlevel base or a nonvertical block tend to accumulate and can become significant, particularly for blocks lying near the boundary between the clear and shaded regions of Fig. 10. In this case the two-dimensional bouncing model should be used, although, as discussed in the section headed "Block with $h/b = 2$," the response of such blocks appears to be very sensitive indeed to the value of e.

For very short blocks, e.g. cubes, the three-dimensional bouncing model is required, and the "correct" kinematic conditions should be used. In this context, the importance of corner impact rather than impact along a full edge has been identified; slip during such collisions can produce significant changes. In general, it is not known a priori which type of impact should be considered, because this depends on tiny imperfections that are practically impossible to spot in advance. Therefore engineers need to be aware that the impact response of short blocks is difficult to predict; a probabilistic approach has to be considered.

Our fairly simple treatment of collisions in the sections on two- and three-dimensional bouncing, which permits consideration of different kinematic conditions—within certain limits—appears to work satisfactorily for the problems that have been investigated, but it has been assumed that slip occurs always in the direction of the grooves and, furthermore, that slip reversal does not occur. It would appear from the section headed "Block with $h/b = 1$" that the first assumption may not be satisfied. This is an area for further work. It is also worth noting that putting a series of parallel

grooves on the impact surfaces has created nearly as many problems as it eliminated.

During our work we have found that authors have referred to the angular velocity ratio (3) as a "coefficient of restitution," and felt free to give it any value that would produce a good fit with experimental response. We find this approach quite confusing; first because the coefficient of restitution e is a well-established semiempirical way of handling normal collisions. The use of a tangential coefficient of restitution, of which we have made a little use in this paper, is already slightly dubious because tangential velocities of different sign during the approach and rebound phases of a collision raise the issue of slip reversal (Stronge 1990). An extension of this approach to angular velocities is, actually, not very useful. If there is no restitution, the value of r depends on geometrical parameters only, and hence is a constant for a given block. If, on the other hand, restitution of one or more velocity components is to be considered, then r can be defined only for a particular collision, because its value depends on the linear velocity of the block before the impact, as well as its geometry and e value.

Acknowledgments

We are grateful to R. J. Denston for assistance in the experimental work. We thank C. R. Calladine, K. L. Johnson, and W. J. Stronge for helpful discussions and comments on an earlier version of this paper. We thank the two anonymous referees for constructive suggestions on the presentation of the paper. Financial support from the Cambridge Commonwealth Trust (P.R.L.) is gratefully acknowledged.

Appendix I. References

Aslam, M., Godden, W. G., and Scalise, D. T. (1980). "Earthquake rocking response of rigid bodies." *J. Struct. Engrg.*, ASCE, 106(2), 377–392.
Brach, R. M. (1989). "Rigid body collisions." *J. Appl. Mech.*, 56, 133–138.
Fowler, H. N., and Stillwell, R. (1932). *Results of excavations conducted by the American school of classical studies at Athens, Vol. 1*, Harvard University Press, Cambridge, Mass., 120.
Goldsmith, W. (1960). *Impact*. Edward Arnold, London, England.
Goldstein, H. (1980). *Classical mechanics*, 2nd Ed., Addison Wesley, Cambridge, Mass.
Housner, G. W. (1956). "Limit design of structures to resist earthquakes." *Proc., World Conf. Earthquake Engrg.*
Housner, G. W. (1963). "The behaviour of inverted pendulum structures." *Bull. Seis. Soc. Amer.*, 53(2), 403–417.
Ishiyama, Y. (1982). "Motions of rigid bodies and criteria for overturning by earthquake excitations." *Earthquake Engrg. and Struct. Dynamics*, 10, 635–650.
Johnson, K. L. (1983). "The bounce of 'superball.'" *Int. J. Mech. Engrg. Ed.*, 11, 57–64.
Johnson, K. L. (1985). *Contact mechanics*. Cambridge University Press, Cambridge, England.
Kilmister, C. W. and Reeve, J. E. (1966). *Rational mechanics*. Longman, London, England.
Lipscombe, P. R. (1990). "Dynamics of rigid block structures," PhD Thesis, University of Cambridge, Cambridge, England.
Lipscombe, P. R., and Pellegrino, S. (1989). "'Rocking' of rigid-block systems under dynamic loads." *Appl. Solid Mech., 3*, I. M. Allison and C. Ruiz, eds., Elsevier Applied Science, New York, N.Y., 175–189.
Maw, N., Barber, J. R., and Fawcett, J. N. (1981). "The role of elastic tangential compliance in oblique impact." *J. Lubrication Tech.*, 103(Jan.), 74–80.

Muto, K., Umemura, H., and Sonobe, Y. (1960). "Study of the overturning vibrations of slender structures." *Proc., 2nd World Cong. Earthquake Engrg.*, Tokyo, Japan, 1239–1261.
Olsen, B. E., Neylan, A. J., and Gorholt, W. (1976). "Seismic test on a one-fifth scale HTGR core model." *Nuclear Engrg. Des.*, 36, 355–365.
Priestley, M. J. N., Evison, R. J., and Carr, A. J. (1978). "Seismic response analysis of structures free to rock on their foundations." *Bull. of the New Zealand Seis. Soc. for Earthquake Engrg.*, 11(3), 141–150.
Routh, E. J. (1877). *Dynamics of a system of rigid bodies*, 3rd Ed., Macmillan, London, England.
Shenton, H. W., and Jones, N. P. (1991). "Base excitation of rigid bodies: formulation." *J. Engrg. Mech.*, 117(10), 2286–2306.
Sinopoli, A. (1987). "Dynamics and impact in a system with unilateral constraints the relevance of dry friction." *Meccanica*, 22, 210–215.
Spanos, P. D., and Koh, A. S. (1984). "Rocking of rigid blocks during harmonic shaking." *J. Engrg. Mech.*, 110(11), 1627–1642.
Stronge, W. J. (1990). "Rigid body collisions with friction." *Proc., Royal Society of London*, England, A, 431, 169–181.
Tso, W. K., and Wong, C. M. (1989). "Steady state rocking response of rigid blocks. Part 1: analysis." *Earthquake Engrg. and Struct. Dynamics*, 18, 89–120.
User's guide, Matlab. (1985). The Mathworks Inc., South Netick, Mass.
Yim, S. C. S., and Lin, H. (1991). "Nonlinear impact and chaotic response of slender rocking objects." *J. Eng. Mech.*, 117, 2079–2100.

Appendix II. Notation

The following symbols are used in this paper:

A, B, C, D = base corner of block;
b = half-width of block;
e = coefficient of restitution;
F_X, F_Y, F_Z = components of impulsive force;
G = center of mass;
g = acceleration due to gravity;
h = half-height of block;
I = moment of inertia about G (two-dimensional model, hence block treated as lamina);
I_x, I_y, I_z = principal moments of inertia;
R = $\sqrt{b^2 + h^2}$;
r = angular-velocity ratio;
X, Y, Z = system of cartesian space coordinates (inertial reference frame);
x, y, z = system of cartesian body coordinates = principal axes of inertia;
α = critical rotation of block (under static conditions, block overturns if $|\theta| > \alpha$);
θ = rotation of block in two-dimensional model (also, observed rotation in three-dimensional model);
Φ, Θ, Ψ = Eulerian angles;
ω_x, ω_y, ω_z = components of angular velocity with respect to body axes;
$\dot{(\ )}$, $\ddot{(\ )}$ = $(d/dt)(\ )$, $(d^2/dt^2)(\ )$; and
$(\ )'$, $(\ )''$ = values of $(\ )$ before and after impact, respectively.